LIQUID CRYSTALS, VOL. 30, NO. 11, NOVEMBER, 2003, 1335–1342

Experimental study of the director pattern dynamics in the vicinity of the Fréedericksz twist geometry

L. N. GONÇALVES†‡, J. P. CASQUILHO‡§, A. C. RIBEIRO†¶ and J. L. FIGUEIRINHAS†¶*

†Centro de Física da Matéria Condensada, Complexo Interdisciplinar da Universidade de Lisboa, Avenida Professor Gama Pinto, 2, 1649-003 Lisboa, Portugal

‡Departamento de Física, Faculdade de Ciências e Tecnologia, Universidade Nova de Lisboa, Quinta da Torre, 2829-516 Caparica, Portugal

§CENIMAT, Faculdade de Ciências e Tecnologia, Universidade Nova de Lisboa, Quinta da Torre, 2829-516 Caparica, Portugal

¶Departamento de Física, Instituto Superior Técnico, Universidade Técnica de Lisboa, 1049-001 Lisboa, Portugal

(*Received 10 February 2003; in final form 4 June 2003; accepted 14 June 2003*)

We present an experimental study of the transient periodic structures appearing in the nematic director field in the magnetically induced reorientation of the director in the vicinity of the twist Fréedericksz geometry. Thin nematic samples (50 μm thick) were exposed to magnetic fields of variable intensity and orientation relative to the surface aligning direction of the sample. The director reorientation was induced by a rapid rotation of the sample in the static magnetic field producing a misalignment between the director and the magnetic field. The director field was optically monitored during the reorientation process and the transient periodic structures were characterized. Two types of periodic structures could be identified, namely bands and walls. Walls grow from bands close to the twist Fréedericksz geometry. The time dependence of the wave length and inclination of the periodic structures was obtained as a function of the magnetic field intensity and orientation relative to the surface aligning direction of the sample. The results for the bands are compared with the predictions of a model that we specifically developed to account for the non-orthogonal field orientations. It is seen that our model can account rather well for the experimental results considering that it uses only the field rotation time as adjustable parameter. All other model parameters are known.

1. Introduction

The subject of transient periodic structures arising in the magnetically induced director reorientation in Fréedericksz geometries has received considerable attention [1–9]. Being an example in which non-equilibrium systems spontaneously develop a complex structure due to their high non-linear nature [10], it constitutes an interesting subject in its own right. Several experimental studies have focused on the Fréedericksz twist geometry case [2, 3, 5–7] whereas the non-orthogonal geometries have been much less studied [11–13]. Theoretical studies based on linear dynamical stability analysis have predicted that the occurrence of bands is favoured for angles above a critical value that can fall well below the orthogonal condition between the magnetic field and the unperturbed director [12]. Also the amplitude of the transient periodic modes should become damped after a critical time and eventually fade away, the faster the more the magnetic field acts away from the normal to the initial director [13]. In our experiments, following a rapid rotation of a nematic cell of 5CB in a constant magnetic field, the director field was optically monitored during the reorientation process and the transient periodic structures were characterized. During the reorientation of the sample, the nematic director field lags behind due to the low viscosity of 5CB. This effect is more significant as the magnetic field becomes more intense. This means that the effective angle of rotation, $\alpha_{ef}=(\pi/2+\beta_{ef})$, of the director field is smaller than the (actual) angle of rotation $\alpha=(\pi/2+\beta)$ (see figure 1) of the sample in the magnetic field, and that the difference between α_{ef} and α becomes more pronounced as the magnetic field intensity is increased.

*Author for correspondence; e-mail: figuei@cii.fc.ul.pt

Liquid Crystals ISSN 0267-8292 print/ISSN 1366-5855 online © 2003 Taylor & Francis Ltd
http://www.tandf.co.uk/journals
DOI: 10.1080/02678290310001605901

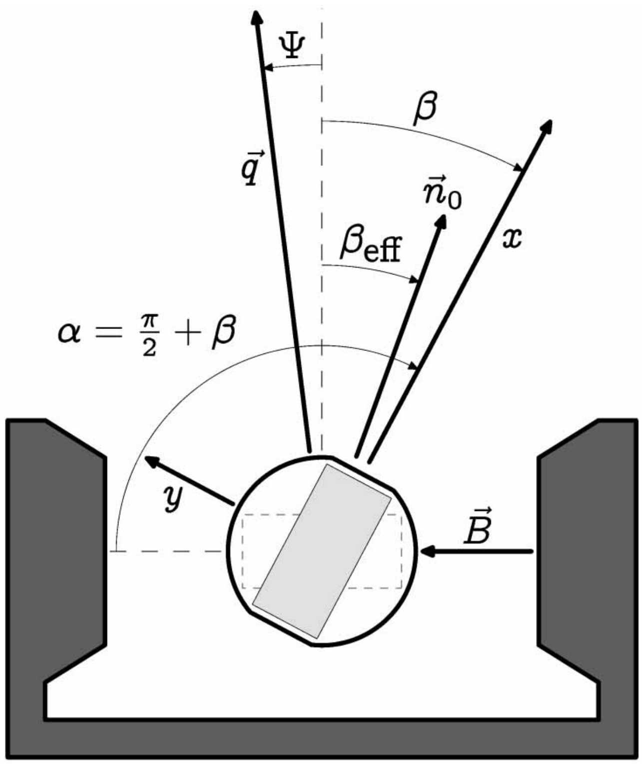

Figure 1. Schematic representation of the experimental assembly. The electromagnet inter-pole space is only 1 mm greater than the diagonal line of the samples. The angle between the axes of the light bulb and of the video camera is about 20°. The rotor and the video camera are both outside the influence of the magnetic field. The light bulb supplies white light polarized vertically. The Faraday effect is not relevant. The angle of rotation of the sample is $\alpha = \pi/2 + \beta$, with β assuming both positive and negative values. ψ is the band wave vector inclination angle relative to the normal to **B**.

The model developed specifically to account for the experimental results presented in this work, allows us to obtain numerical results using the viscoelastic parameters of 5CB [14]. This model is a generalization of the perturbation methods developed in [12] and [13]. It is based on the study of the stability of the full solution for the non-periodic director field reorientation with respect to periodic perturbations. A periodic pattern that is tilted with respect to the initial orientation of the director is found, in agreement with our experimental results. The amplitude of the periodic perturbation only grows significantly near the orthogonal geometry, predicting that the bands should only be observable in the vicinity of the Fréedericksz geometry. This is also in agreement with our experimental results. Two modes are observed experimentally. One corresponds to the linear mode, predicted by our model. There is also a non-linear mode, with a smaller wave vector, according to a model developed by Srajer *et al.* [3] for the orthogonal condition, based on the numerical solution of non-linear dynamic equations. Both the numerical and the experimental results give a consistent picture of the reorientation dynamics of the nematic director.

2. Experimental

Figure 1 shows schematically the architecture of our experimental assembly. The magnetic field is produced by a VARIAN V-7400 electromagnet, is cooled by a heat exchanger V-7873, and regulated by a VARIAN FIELDIAL MARK I power source. The magnetic induction can reach 2 T. Rectangular $12 \times 25\,\text{mm}^2$ cells with two 0.7 mm thick glasses and a 50 µm gap, manufactured by E.H.C.Co., were used. The angle of azimuthal anchorage is 1° relative to the direction of the longest edges of the cells. The cells are filled with 5CB (4-*n*-pentyl-4′-cyanobiphenyl). The sample is illuminated with a halogen light bulb with a power of 55 W. The light is polarized linearly on the incidence plane. The angle of incidence is equal to the observation angle (about 10°). A colour video camera JVC TK-1281EG, a GENIUS VIDEO WONDER PRO II V2 video capture board and a 400 MHz PENTIUM II with 90 Mbyte of RAM allowed the capture of films at a sustained rate of 25 frames per second. The samples are fixed to a massive load that is connected to a mechanical rotor. This rotor allowed the rotation of the sample inside the magnetic field in ≈30 ms and with a resolution of 0.24° around an axis normal to the cell plane.

To determine the orthogonal condition between the unperturbed director and the magnetic field, the sample is fixed such that the longer edges are perpendicular to the magnetic field, and the sample orientation that leads to the formation of periodic structures with minimum intensity of the magnetic field when switching on the electromagnet is found. Based on the obtained reference alignment, the low and high limit angles for the sample rotation are defined in the rotor. The total rotation angle $\alpha = \pi/2 + \beta$ has a systematic uncertainty of 1°. The sample temperature is kept at 26°C.

With the magnetic field off, the sample is oriented with the unperturbed director along the magnetic field direction. Next the magnetic field is raised to the desired value and, after a convenient stabilization time interval, the director reorientation process is initiated by rotating the rotor carrying the sample to the desired angle β. The video system records the samples image during the process. ψ is the average angle between the wave vector of the periodic mode and the normal to the magnetic field.

3. Data and analysis

Periodic structures in the director field as shown in figure 2 are only observable in the vicinity of the twist geometry within the margin $-0.5^\circ < \beta < 4.5^\circ$ and for fields higher than 2.1 B_C where $B_C = 1.141$ kG and is the twist Fréedericksz transition critical field for our system. The observation of the time evolution of the periodic structures during the reorientation process shows two distinct behaviours. In one case the periodic structures (here referred to as bands) become visible during the reorientation process but then fade away in a relatively short time as predicted by Casquilho and Figueirinhas [13]. In the other case they appear and later become more pronounced, remaining for longer times after the reorientation process without fading away. These latter structures have evolved from the bands into walls as pointed out in [15] as a result of the steady growth of the band amplitude appearing at early times. The average orientation of the periodic structures is dependent upon β and the magnetic field intensity. It is possible to observe that it varies slightly during the reorientation process but the wave vector points predominantly in the x axis direction. The time evolution of the periodic structures can be better characterized through the time evolution of the Fourier transform of the images of the structures, and since the structures wave vector is within 20° of the x axis direction, the evolution of the structures is well depicted by a representation of their Fourier components projected in the x axis as function of time, as shown in figure 3. It is seen that after the initial fast misalignment between the magnetic field and the unperturbed director, the reorientation process of the director begins and a mode of high wave vector appears, reaches a maximum amplitude and begins to fade away. During this process another mode with a smaller wave vector appears and does not vanish in the same time scale as the former mode. The mode with the higher wave vector corresponds to the band structures and is the linear mode [3], while the second mode is associated with the walls and is the non-linear mode [3]. For the structures with higher $|\psi|$ values the second mode amplitude remains small and so only the bands are clearly seen. A typical example of this behaviour is seen in figure 3. During the reorientation process the mode of higher wave vector associated with the bands reaches maximum amplitude at a certain time t_m. The values of the wave vector amplitude and orientation recorded at t_m, as well as t_m, are registered for each value of β and of the magnetic field intensity. These results are compared with simulations obtained from a model that we specifically developed for the non-homogeneous reorientation of the director in the non-orthogonal condition between the magnetic field and the unperturbed director that we will now describe.

The model analyses the reorientation of the director

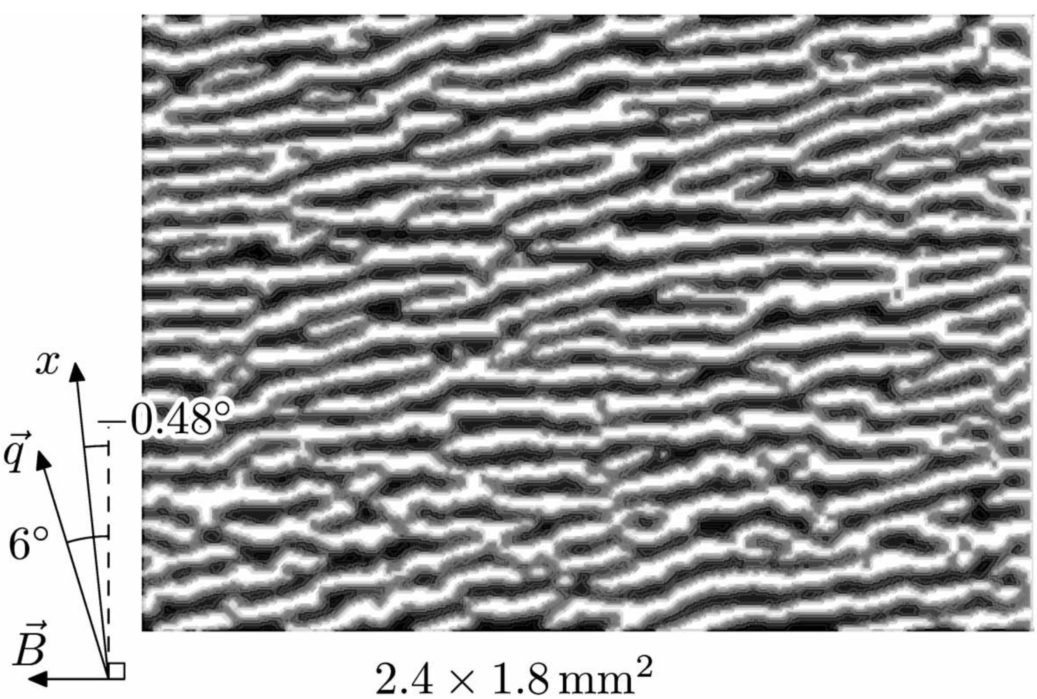

Figure 2. Picture of the stripe pattern for $\mathbf{B} = 5$ kG, $\beta = -0.48^\circ$ and $\psi = +6^\circ$.

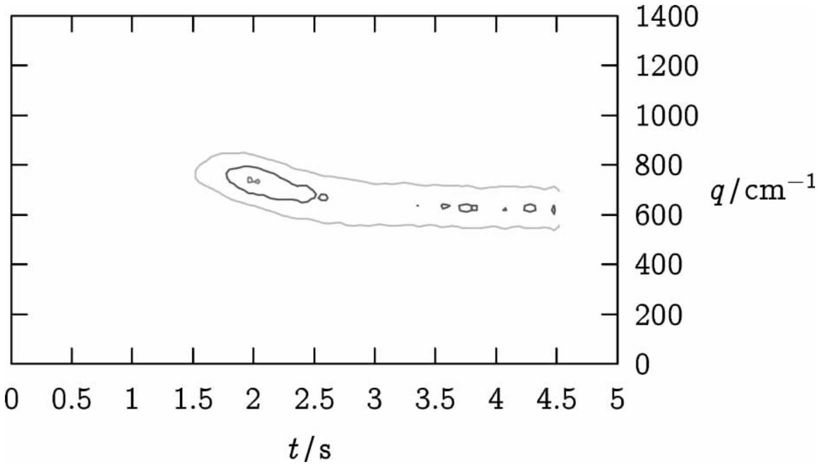

Figure 3. Fourier components of the periodic structure projected on the x axis as function of time. Obtained at $\mathbf{B}=4.56$ kG and $\beta=+0.48°$, $t_m=1.98$ s.

in the twist geometry for the non-orthogonal condition between the magnetic field and the unperturbed director. The angle between the initial director and the magnetic field is time dependent during the initial sample rotation. The time to complete this initial sample rotation τ_r is the only adjustable parameter of our model, all other parameters are known. The model performs a dynamical stability analysis of the full non-linear solution for the homogeneous director field reorientation in the frame of the Ericksen–Leslie theory [16]. It considers a periodic perturbation of the homogeneous time dependent director and evaluates its time evolution during the director reorientation process. The director, fluid velocity and magnetic field are, respectively:

$$\begin{aligned}\mathbf{n}&=cos\,[\theta(x,y,z,t)]\hat{e}_x+\sin\,[\theta(x,y,z,t)]\hat{e}_y\\ \mathbf{v}&=v_x(x,y,z,t)\hat{e}_x+v_y(x,y,z,t)\hat{e}_y\\ \mathbf{H}&=H\left\{\cos\left(\pi/_2+\beta\right)\hat{e}_x+\sin\left(\pi/_2+\beta\right)\hat{e}_y\right\}\end{aligned}\tag{1}$$

with θ, v_x and v_y given by:

$$\begin{aligned}\theta(x,y,z,t)&=\theta_0(t)\cos(q_zz)+\xi_\theta(t,\mathbf{q})\cos\left(q_xx+q_yy\right)\cos(q_zz)\\ v_x(x,y,z,t)&=-\xi_v(t,\mathbf{q})q_y\sin\left(q_xx+q_yy\right)\cos(q_zz)\\ v_y(x,y,z,t)&=\xi_v(t,\mathbf{q})q_x\sin\left(q_xx+q_yy\right)\cos(q_zz)\end{aligned}\tag{2}$$

in which $q_z=\pi/d$ where d is the sample thickness, $\theta_0(t)$ is the amplitude of the homogeneous reorientation, $\xi_\theta(t,\mathbf{q})$ is the amplitude of the periodic perturbation superimposed with wave vector $\mathbf{q}=q_x\hat{e}_x+q_y\hat{e}_y$. $\xi_v(t,\mathbf{q})$ is the velocity amplitude associated with the periodic perturbation.

The initial amplitudes of the aperiodic and periodic modes are evaluated according to a thermal distribution [3]. The perturbation is seen to reach the maximum amplitude at a specific time $t_m(\tau_r, \mathbf{H}, d, \alpha_i, K_j, \chi_a)$ and subsequently decays. The wave vector $q_m(t_m, \tau_r, \mathbf{H}, d, \alpha_i, K_j, \chi_a)$ that maximizes the perturbation recorded at the time t_m and $t_m(\tau_r, \mathbf{H}, d, \alpha_i, K_j, \chi_a)$ are compared with the experimental results. α_i are the five independent Leslie viscosity coefficients and K_j are the three Frank elastic constants. Details of the model are presented elsewhere [17, 18].

Contour plots of the band wave vector inclination as a function of β and the magnetic induction are shown in figure 4. The asymmetry between positive and negative values of β, is due to the finite rotation time τ_r of the sample. During this rotation the director lags behind from which results $\beta_{ef}<\beta$. This allows us to interpret the full curve of figure 4 as the $\beta_{ef}=0$ curve, since $\mathbf{q}\|\mathbf{n}_0$ in the orthogonal condition between $\mathbf{B}$ and $\mathbf{n}_0$ [3, 15, 17]. The inclination of the band wave vector, as measured by ψ, increases when β_{ef} departs from zero at constant magnetic induction. In figure 5 the curve shown in figure 4 is compared with the theoretical result produced by the model for bands with wave vector along the initial director, considering a rotation time of 20 ms. The experimental curve was shifted by $+0.7°$ to match the theoretical curve, allowing the determination of the offset rotation angle which is then $+0.7°$. The two curves agree rather well considering that the model uses τ_r as the only adjustable parameter. (In figures 4, 7 and 8 the offset rotation angle is included in the β values.)

Figure 6 compares the wave vector amplitudes as a function of the magnetic induction for $\beta=0$ given by our model and the model introduced by Srajer et al. [3]. The full curve is the result of the model for the band wave vector dependence and the two sets of points are the results for the linear and non-linear modes wave vector produced by Srajer's model for the reorientation in the orthogonal field condition. A better agreement

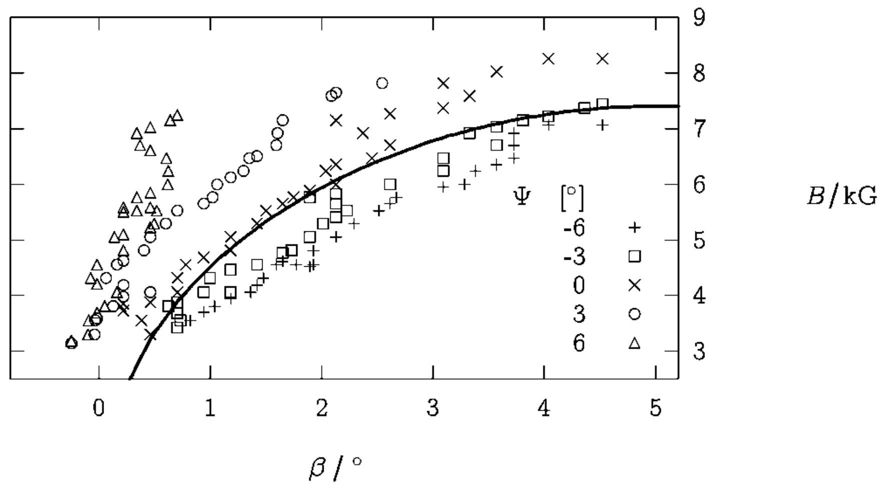

Figure 4. Points corresponding to $\psi=-6°$, $-3°$, $0°$, $3°$, and $6°$ obtained from the contour plots of the experimental surface $\psi(\beta,\mathbf{B})$. An asymmetry between positive and negative values of β can be seen (see text). The full curve is a polynomial fit to the data corresponding to bands with wave vector parallel to the initial director. The ψ values are measured from the films using a Hough transform technique [19].

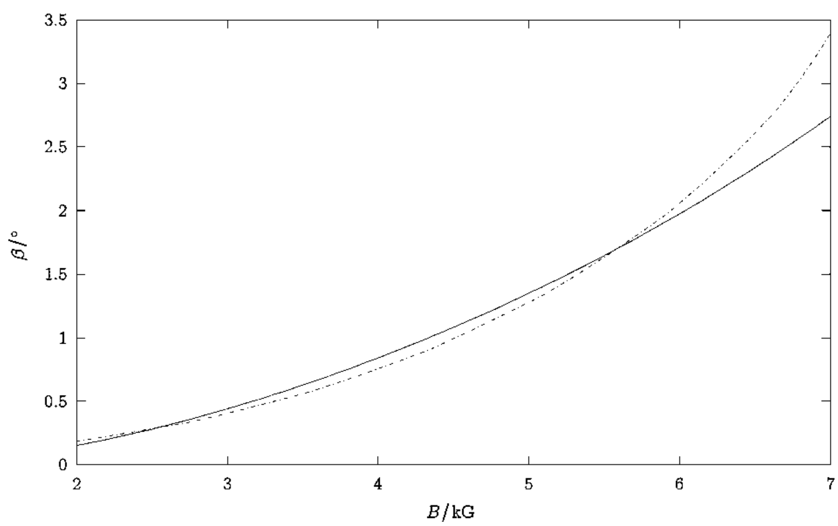

Figure 5. Comparison between the experimental and theoretical results regarding the bands with wave vector parallel to the initial director as a function of the magnetic induction. The full curve is the theoretical result produced by the model considering a rotation time of 20 ms, the dashed line is the polynomial fit shown in figure 4.

between the results of our model and the linear mode of Srajer's model would be expected, but we believe that the main reason for the observed discrepancy is Srajer's model does not consider the initial misalignment time between the initial director and the magnetic field, which is taken into account in our model. For the reorientation of the nematic polymer considered in Srajer's work [3], short misalignment times (below 0.05 s) may be neglected [18] but this is not the case for the liquid crystal used in this study as shown by our data (figure 4).

Figure 7 shows the magnetic induction dependence of the wave vector amplitude determined experimentally (crosses from the linear mode and squares from the non-linear mode) and predicted by our model (lozenges) for $\beta=+0.22°$. Similar dependences are found for other values of β, as it is found that at constant field the wave vector amplitude is weakly dependent upon β for the ranges studied. There is good agreement between the experimental results and the predictions of our model within the accuracy of the experimental results, confirming the model validity to describe the bands properties.

Figure 8 shows the magnetic induction dependence of

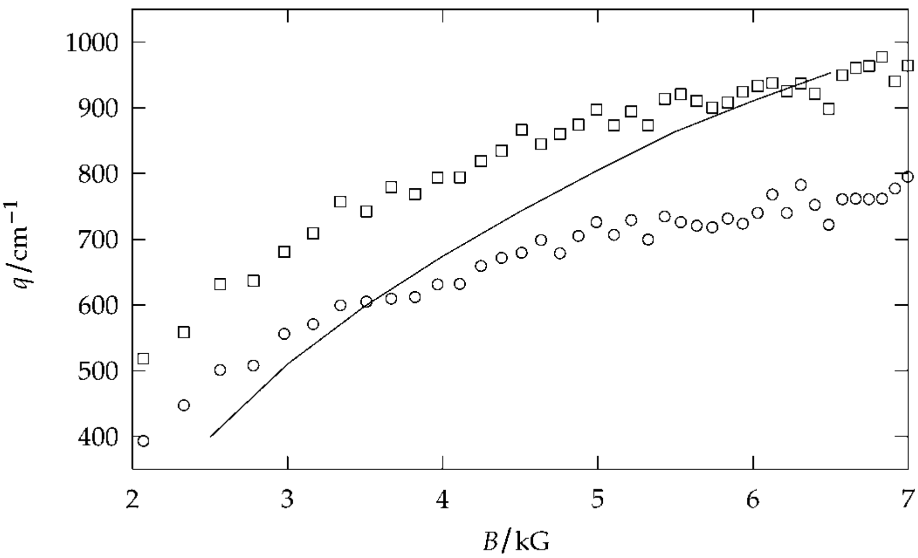

Figure 6. Wave vector amplitude as a function of magnetic induction for $\beta = 0°$, given by our model (full line) and Srajer's model (squares) for the linear (higher wave vector amplitude mode) and (circles) for the non-linear modes.

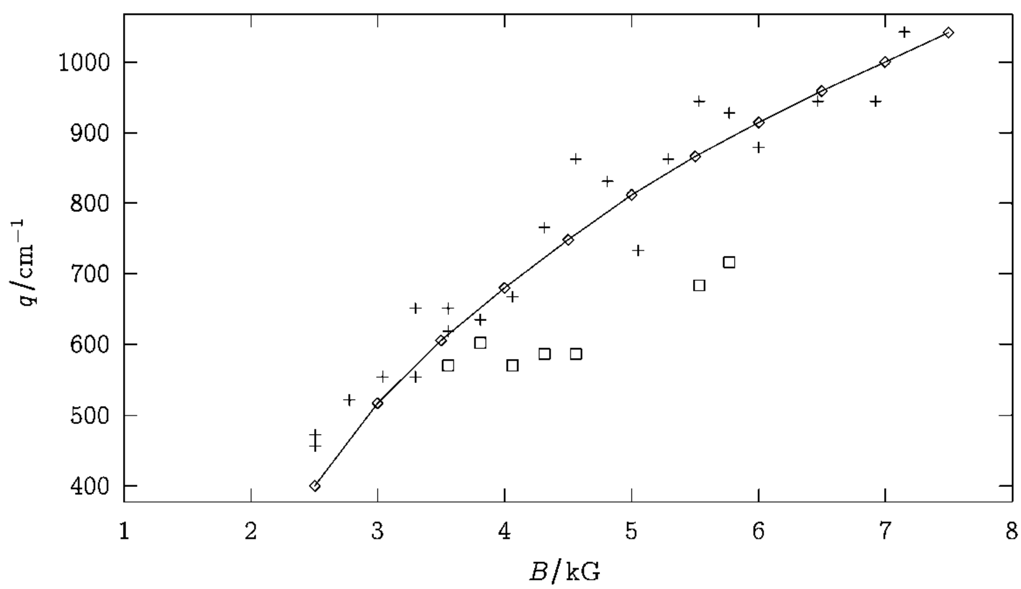

Figure 7. Experimental and theoretical magnetic induction dependence of the wave vector amplitude for $\beta = +0.22°$. Crosses and squares represent, respectively, the linear and non-linear modes wave vector x components. The full curve is our model prediction. Similar dependences are found for other values of β.

time t_m for $\beta = +0.70°$ and $\beta = +0.22°$. The full and dotted curves are our model predictions rescaled by a multiplying factor of 1.35. This discrepancy may be due to a less accurate evaluation of the initial amplitude of the non-periodic and periodic modes that in the first approximation only affects the time t_m. Nevertheless the global behaviour of t_m is captured by the model indicating that the essential aspects of the mechanism behind the formation and evolution of the bands are well described.

4. Conclusions

Two types of transient periodic structure in the nematic director field, namely bands and walls, were experimentally observed during the magnetically induced director reorientation. These structures were

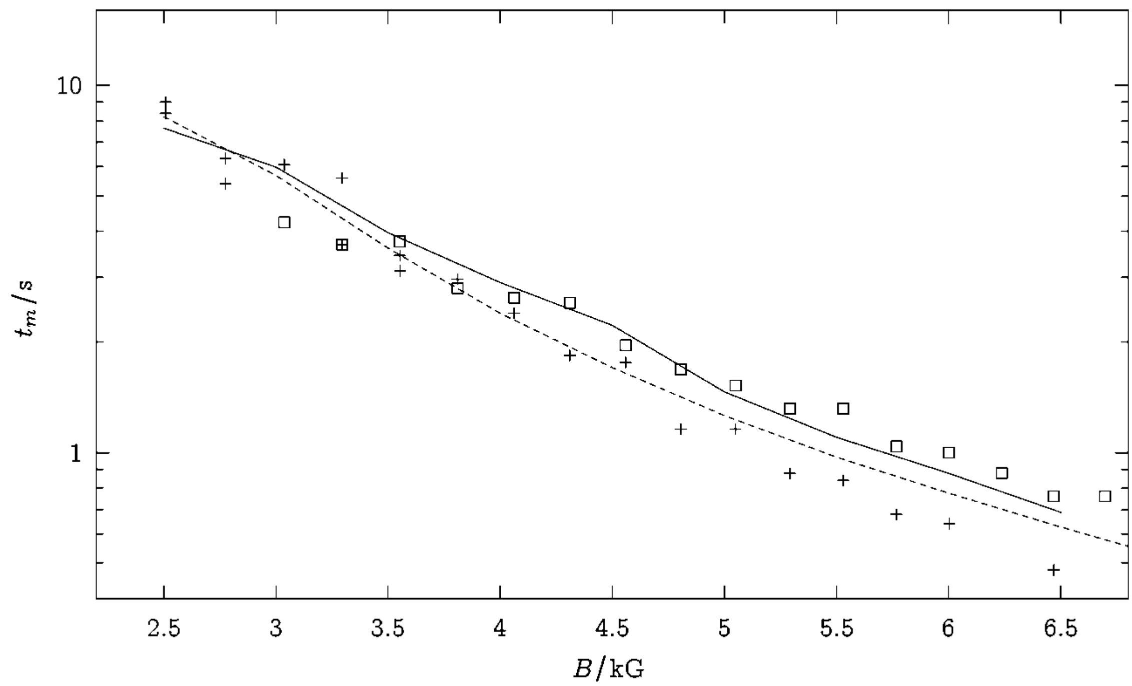

Figure 8. Magnetic induction dependence of time t_m for $\beta = +0.7^\circ$ (squares) and $\beta = +0.22^\circ$ (crosses). The full and dotted curves are our model predictions, respectively, for $\beta = +0.7^\circ$ and $\beta = +0.22^\circ$. The theoretical curves presented are rescaled by a multiplying factor of 1.35 over the model results (see text).

detected in the vicinity of the twist Fréedericksz geometry. When the magnetic field acts significantly away from the normal to the initial director $\mathbf{n}_0$, the amplitude of the bands was damped sufficiently quickly to prevent the formation of the (splay–bend) inversion walls that arise in the Fréedericksz geometry [20]. The band wave vector measured at the time t_m of the maximum mode amplitude grows monotonously with the magnetic field while t_m itself decreases monotonously with the field. The band inclination angle ψ at fixed sample rotation angle β increases with the field. At constant magnetic field, the band inclination increases when the magnetic field acts away from the normal to the initial director, and it vanishes in the orthogonal condition ($\beta_{\mathrm{ef}} = 0$).

The results and simulations presented show that the transient periodic structures arising during the director reorientation in the vicinity of the twist Fréedericksz transition geometry can be well described by a dynamic linear perturbation analysis of the Ericksen–Leslie nematodynamic equations. The analysis carried out also answers the question raised by theoretical studies [12, 13] that predicted the appearance of periodic structures well away from the orthogonal condition between the initial director and the magnetic field. It shows that the bands are only visible in the vicinity of the twist Fréedericksz transition geometry, because the amplitude of the periodic perturbation is very small otherwise. The actual range of values of the angle β in which the periodic structures are observable is limited by the critical value of the angle β [12, 13, 17, 18] and depends upon the sensitivity of the optical set-up.

We acknowledge project POCTI/34453/CTM/2000 for financial support.

References

[1] Guyon, E., Meyer, R., and Salan, J., 1979, *Mol. Cryst. liq. Cryst.*, **54,** 261.
[2] Lonberg, F., Fraden, S., Hurd, A. J., and Meyer, R. B., 1984, *Phys. Rev. Let.*, **52,** 1903.
[3] Srajer, G., Fraden, S., and Meyer, R. B., 1989, *Phys. Rev. A*, **39,** 4828.
[4] Kini, U. D., 1991, *J. Phys II Fr.*, **1,** 225.
[5] Grigutsch, M., Klöpper, N., Schmiedel, H., and Stannarius, R., 1994, *Phys. Rev. E*, **49,** 5452.
[6] Pashkovsky, E. E., Stille, W., and Strobl, G., 1995, *J. Phys. II Fr.*, 397.
[7] Simões, M., and Palangana, A. J., 1999, *Phys. Rev. E*, **60,** 3421.
[8] Krzyzansky, D., and Derfel, J., 2000, *Phys. Rev. E*, **61,** 6663.
[9] Kini, U. D., 1992, *Liq. Cryst.*, **12,** 449.
[10] San Miguel, M., Amengual, A., and Hernandez-Garcia, E., 1994, *Phase Transitions*, **48,** 66.
[11] Karn, A., Shen, Y. R., and Santamato, E., 1990, *Phys. Rev. A*, **41,** 4510.
[12] Casquilho, J. P., 1999, *Liq. Cryst.*, **26,** 517.

[13] CASQUILHO, J. P., and FIGUEIRINHAS, J. L., 2002, *Liq. Cryst.*, **29,** 127.
[14] BUKA, A., and KRAMER, L., 1996, *Pattern Formation in Liquid Crystals* (Springer).
[15] GRIGUTSCH, M., KLÖPPER, N., SCHMIEDEL, H., and STANNARIUS, R., 1995, *Mol. Cryst. Liq. Cryst.*, **261,** 283.
[16] DE GENNES, P. G., and PROST, J., 1993, *The Physics of Liquid Crystals* (Oxford: Clarendon Press).
[17] CASQUILHO, J. P., GONÇALVES, L. N., and FIGUEIRINHAS, J. L. *Mol. Cryst. Liq. Cryst.* (to be published).
[18] FIGUEIRINHAS, J. L., and CASQUILHO, J. P. (to be published).
[19] GONZALEZ, R. C., and WINTZ, P., 1987, *Digital Image Processing* (Addison-Wesley).
[20] CASQUILHO, J. P., GONÇALVES, L. N., and MARTINS, A. F., 1996, *Liq. Cryst.*, **21,** 651.